Title: The evolution of white-tailed jackrabbit camouflage in response to past and future seasonal climates

Authors: Mafalda S. Ferreira[1,2,3,*,¶], Timothy J. Thurman[3], Matthew R. Jones[3], Liliana Farelo[1], Alexander V. Kumar[4,5], Sebastian M. E. Mortimer[3], John R. Demboski[6], L. Scott Mills[4,7], Paulo C. Alves[1,2,4,8], José Melo-Ferreira[1,2,8,*,‡], Jeffrey M. Good[3,4,*,‡]

Affiliations:

[1]CIBIO, Centro de Investigação em Biodiversidade e Recursos Genéticos, InBIO Laboratório Associado, Universidade do Porto; Vairão, Portugal.

[2]Departamento de Biologia, Faculdade de Ciências da Universidade do Porto; Porto, Portugal.

[3]Division of Biological Sciences, University of Montana; Missoula, Montana, United States of America.

[4]Wildlife Biology Program, College of Forestry and Conservation, University of Montana; Missoula, Montana, United States of America.

[5]U.S. Fish and Wildlife Service, Fort Collins, Colorado 80526, United States of America.

[6]Zoology Department, Denver Museum of Nature & Science; Denver, Colorado, United States of America.

[7]Office of Research and Creative Scholarship, University of Montana; Missoula, Montana, United States of America.

[8]BIOPOLIS Program in Genomics, Biodiversity and Land Planning, CIBIO, Vairão, Portugal.

*Correspondence to: sferreira.mafalda@gmail.com (M.S.F); jmeloferreira@cibio.up.pt (J.M.-F.); jeffrey.good@umontana.edu (J.M.G)

¶ Current address: Department of Medical Biochemistry and Microbiology, Uppsala University, Uppsala, Sweden

‡ Shared senior authorship

Abstract:

The genetic basis of adaptive traits has rarely been used to predict future vulnerability of populations to climate change. We show that light versus dark seasonal pelage in white-tailed jackrabbits (*Lepus townsendii*) tracks snow cover and is primarily determined by genetic variation at Endothelin Receptor B (*EDNRB*), Corin Serine Peptidase (*CORIN*), and Agouti Signaling Protein (*ASIP*). Winter color variation was associated with deeply divergent alleles at these genes, reflecting selection on both ancestral and introgressed variation. Forecasted reductions in snow cover are likely to induce widespread camouflage mismatch. However, simulated populations with variation for darker winter pelage are predicted to adapt rapidly, providing a trait-based genetic framework to facilitate evolutionary rescue. These discoveries demonstrate how the genetic basis of climate change adaptation can inform conservation.

One-Sentence Summary: Future adaptation to snow cover depends on standing genetic variation for winter camouflage in white-tailed jackrabbits.

Preservation of genetic diversity is a primary goal of conservation biology (*1*), reflecting the critical role that genetic variation plays in promoting rapid adaptation to environmental change (*2*, *3*). While there has been progress in dissecting the genetic basis of adaptation in some species (*4–6*), rarely has such information been used to guide the conservation of populations (*7*, *8*). These shortcomings reflect the difficulties of genetic mapping in natural populations (*9*) and using genotype-to-phenotype maps to facilitate adaptive responses (*7*).

Circannual shifts in morphology, physiology, and behavior cued by changes in photoperiod allow many species to buffer the challenges of seasonal environments (*10*). Seasonal molts to winter-white pelage and plumage have evolved in at least five animal families to maintain crypsis in snow-covered environments (*11*). Winter coloration has been directly tied to survival in snowshoe hares (*12*, *13*) and several species appear vulnerable to camouflage mismatch caused by global snow cover declines (*14–18*). We examined how snow cover variation has shaped the evolution and future adaptive potential of winter camouflage in white-tailed jackrabbits (*Lepus townsendii*), a North American species undergoing widespread population declines (*19*).

Winter coat color tracks variation in snow cover across the white-tailed jackrabbit range

Winter coat color varies from brown to white across the white-tailed jackrabbit distribution (*11*, *20*). We used 1312 georeferenced records to estimate a species distribution model (Fig. 1 and Fig. S1 and S2A) (*21*), and used climate covariates and 196 museum specimens with mostly white or brown pelage to build a probabilistic model of winter coloration across the range (Fig. 1A, Tables S1 and S2).

Consistent with previous work (*11*), the probability of an animal having white pelage increased with snow cover duration and a correlate of snow seasonality (mean diurnal temperature range) and decreased with an index of snow transience (isothermality; Table S1). Our model predicted a mosaic of winter-white or -brown populations separated by zones of intermediate coat color probabilities. We found a steep winter color gradient between the Rocky Mountains and the Great Plains of Colorado (Fig. 1C), which included a previously described population with continuous coat color variation (*20*).

The genetic basis of winter coat color

To dissect the genetic basis of winter color variation, we sequenced (62.5×; Table S3, Data S1 and S2) and assembled a white-tailed jackrabbit genome (48.03 Mb scaffold N50; Table S3). We also sequenced 74 genomes from the coat color polymorphic zone in Colorado (Fig. 1C) to low coverage (~1.8×; Table S4), of which seven genomes were also re-sequenced to moderate coverage (~12.2×; Data S1 and Table S6). Analysis of 239,834 unlinked single-nucleotide polymorphisms (SNPs) showed weak population structure partitioned across two genetic clusters not broadly coincident with coat color variation (Fig. S3E; between-cluster weighted fixation index, F_{ST} = 0.036). Spectrophotometric analysis of six dorsal regions (Fig. S4) uncovered considerable variation in dorsal brightness, hue, and contrast (n=61, 51% variance PC1; Fig. S4, 5A and 5D), variegation (14.6% variance PC2; Fig. S4, 5B and 5E), and mottling (7.5% variance PC3; Fig. S4, 5C and 5F). White versus brown categories used in our binary phenotypic model (Fig. 1) consistently partitioned continuous color variation along PC1 (Fig. S4B). Genome-wide association tests between 5,557,716 SNPs and PC1 of the spectrophotometric data revealed significant associations robust to population structure on two scaffolds, each containing one gene involved in melanogenesis (Fig. 2 and Fig. S6).

One association centered on Corin Serine Peptidase (*CORIN*; Fig. 2B; $P = 7.26 \times 10^{-16}$), a serine peptidase expressed in hair follicles that acts as a downstream suppressor of the Agouti Signaling Protein (*ASIP*) (*22*). Loss-of-function mutations in *CORIN* have been associated with enlarged pheomelanin bands and lighter pelage in tigers (*23*) and mice (*24*). The other association centered on the Endothelin Receptor B (*EDNRB*, Fig. 2D; $P = 3.31 \times 10^{-22}$), a G-protein coupled receptor essential to developmental migration and differentiation of melanocyte precursors (*25*, *26*). *EDNRB* mutations cause white piebald spotting due to absence of melanocytes (*27*). For both genes, top associated variants were non-coding, consistent with a regulatory basis of seasonal camouflage variation.

We also performed association tests on all 74 jackrabbits, binning color as white or brown, and found two additional associations. One overlapped a non-coding region ($P = 1.29 \times 10^{-14}$; Fig. S6B and S7) near genes from the alpha-2-macroglobulin gene family, which have been linked to reproduction (*28–30*), and may reflect a correlated seasonal trait. The other overlapped *ASIP* ($P = 1.38 \times 10^{-14}$; Fig. 6B), a well-known signaling protein that shifts melanogenesis to lighter phaeomelanin production or inhibits pigment production (*31*). *ASIP* has been associated with discrete winter coat color polymorphisms in snowshoe and mountain hares (*6*, *32*).

We next used mass spectrometry to generate high confidence genotypes for 59 jackrabbits with spectrophotometric data at 34 linked SNPs (average within-gene $r^2 \geq 0.93$) across *CORIN* (n=13), *EDNRB* (n=9), and *ASIP* (n=12) (Fig. S8; Data S1 and S3). *CORIN* ($P = 6.82 \times 10^{-9}$) and *EDNRB* ($P = 7.73 \times 10^{-12}$) alleles remained strongly associated with PC1 (Tables S7 and S8), showing largely additive (Fig. 2C, E; all $P > 0.05$, dominance deviation test; Tables S9, and S10) and independent effects ($P > 0.05$; Fig. 2F, Fig. S9; Table S11). *ASIP* was not associated when including the other genes as covariates (Tables S7 and S8), but we detected

epistatic interactions between the top associated SNPs at *ASIP* and *CORIN* ($P < 0.05$; Table S11), consistent with known molecular interactions between these genes (*22*). A linear model of the top associated SNPs from each gene explained 65% of phenotypic variation (model D, Table S12). While a precise estimate of effect sizes awaits more sampling, winter camouflage in white-tailed jackrabbits appears to be primarily determined by large-effect additive genetic variation at *CORIN* and *EDNRB*, with a minor contribution of *ASIP*.

Multigenic winter camouflage adaptation is shaped by selection on ancient genetic polymorphisms and gene flow between species

Genome-wide comparisons among white-tailed jackrabbit genomes revealed increased scaled absolute genetic divergence between winter-white and winter-brown associated alleles of *CORIN*, *EDNRB*, and *ASIP* (Z-score ≥ 3; Fig.3A and Fig. S10), indicating that seasonal camouflage variation did not arise from recent mutations in white-tailed jackrabbits. To examine the history of these genes, we combined white-tailed jackrabbit genomes with 10 new and 19 previously published (*6*, *32–36*) genomes (~7.5 – 33.5×; Table S6) from nine other *Lepus* species, including four showing seasonal camouflage (Data S1). Genome-wide analysis clustered white-tailed jackrabbits with three other color-changing species (Fig. 3B; Fig. S11; Table S13). *CORIN*, *EDNRB*, and *ASIP* showed discordant local genealogies whereby winter-brown alleles from white-tailed jackrabbits grouped with black-tailed jackrabbits, a winter-brown species, while winter-white alleles grouped with closely related winter-white species (Fig. 3B and Fig. S12). The estimated divergence time between the white and brown haplotypes exceeded three million years (myr) at all three genes [*EDNRB* = 4.2 myr (95% HPD 3.3-5.0 myr); *CORIN* = 3.3 myr (95% HPD 2.9-4.3 myr); *ASIP* = 3.1 myr (95% HPD 2.4-3.7 myr); Fig. S13], suggesting a common ancestor near the onset of *Lepus* diversification (*37*). Deep phylogenetic discordance at

each gene could reflect gene flow from another species (*38*). Consistent with this, divergence across an ~88 kb interval overlapping *ASIP* was reduced between black-tailed jackrabbits and the white-tailed jackrabbit brown allele relative to simulated expectations (Fig. 3C, Fig. S14B-C and Table S14). By contrast, the white allele showed normal levels of divergence to other winter-white hares (Fig. 3D and Fig. S14D). Black- and white-tailed jackrabbits occupy similar prairie habitats with overlapping ranges and show substantial genome-wide introgression (D-statistic = 0.19, $P << 0.0001$; 4% admixture, $P << 0.0001$). The persistence of introgressed alleles, a binary association (Fig. S6B), and a central role in color evolution (*31*) suggest that *ASIP* contributes to a component of color variation not captured by our measurements. This is the third instance of introgression at *ASIP* contributing to winter camouflage in hares (Fig. 3B) (*6*, *32*), suggesting that some genes may be evolutionary hotspots for adaptive introgression (*39*).

The evolutionary processes shaping variation at *CORIN* and *EDRNB* were less clear. Divergence (d_{xy}) between black-tailed jackrabbits and the brown-associated intervals of both genes were not unusually shallow (Fig. 3C), as expected with recent introgression. However, closer inspection revealed local phylogenetic variation consistent with ancient gene flow (Fig. S14). While the causative mutations remain unknown, top associated SNPs at both genes fell outside putative introgression tracts. These patterns suggest a history of recombination among ancient color alleles at *CORIN* and *EDRNB*, likely maintained by long-term spatially varying selection (*40*). Collectively, these findings indicate that multigenic winter camouflage adaptation (Fig. 1), shaped by selection on standing and introgressed variation (Fig. 3), has long been important to white-tailed jackrabbit survival.

Future climate change vulnerability and adaptive potential of seasonal camouflage variation

Seasonal snow cover is predicted to decline over the next century (*41*), which may reduce the adaptive value of winter-white coats (*11*). To understand how jackrabbit camouflage might evolve in response to climate change, we forecasted winter coat color probabilities for the year 2080 based on correlates of snow residence time, seasonality, and transience (Figs. S2D-F, 4A). We used forecasts under a high CO_2 emissions scenario (RCP8.5) to model challenging, though not unlikely (*42*), conditions jackrabbits may experience in the future. Under this model, winter-brown coats ($P_{(brown)} \geq 0.8$) will be strongly favored across much of the southern (USA) range (~49% at $P_{(brown)} \geq 0.8$ in 2080; Fig. S2B, E, F), a 3.1-fold increase over historical conditions (16% at $P_{(brown)} \geq 0.8$). While the rate of mismatch will depend on which emissions scenario transpires, future reductions in snow cover are likely to induce widespread camouflage mismatch (Fig. 4A) given strong correlations of forecasted parameters across emission scenarios (*21*).

Previous work proposed that standing variation for seasonal camouflage could promote rapid evolutionary rescue in species threatened by diminished snow cover (*11*). To understand if the genetic basis of camouflage inferred from Colorado populations may facilitate evolutionary rescue more broadly, we sequenced 69 additional white-tailed jackrabbit genomes from across the range (~2.1×; Table S5). Although winter phenotypes were mostly unknown for these samples, we found low genetic structure (F_{ST} = 0.020 Colorado versus North Dakota; Fig. S15) and color-associated polymorphisms outside of Colorado at all three genes (Fig. S15). Moreover, the presence of white alleles at the three genes was positively correlated with snow cover duration across the range (r = 0.33-0.46, $p < 0.05$; Fig. S16). Therefore, multigenic color-associated variation appears functionally relevant and broadly shared across the range.

Next, we simulated the capacity for populations with the largest forecasted mismatch ($\Delta P_{(brown)}$ = 0.75) to adapt to changes in snow cover. Focusing on large-effect variation at *CORIN* and *EDRNB*, we found that populations without winter-brown alleles trended towards extinction,

while populations with winter-brown alleles could adapt rapidly. Evolutionary rescue was likely even under a high-emissions scenario and when adaptive winter-brown alleles were initially rare (Fig. 4B, Fig. S17 and S18). However, the efficacy of selection depended on genetic dominance. Fully recessive winter-brown variation, as found in other hares (*6*, *32*), was associated with slower responses and larger population declines (Fig. 4B and Fig. S18). Thus, the capacity for evolutionary rescue to buffer against future population declines in this and other species confronted by seasonal mismatch (*11*) will depend on local demography, the genetic architecture of adaptive traits, and frequencies of adaptive alleles (*3*).

Towards a framework for prioritizing and facilitating conservation efforts

Optimism that standing variation could enable evolutionary rescue in the face of camouflage mismatch is tempered by widespread population declines in white-tailed jackrabbits caused by habitat alteration, extermination, shifts in predator communities, and climate change (*19*) coupled with the emerging threat of rabbit hemorrhagic disease virus (*43*). Using regional conservation assessments (*19*), we found that populations predicted to harbor winter-brown variation ($P_{(brown)} \geq 0.8$) have disproportionally experienced local declines or extirpations (Pearson's χ^2 test *P* value = 2.2×10^{-16}; Cramér's V = 0.31; Fig. 4B and Fig. S2C). Given these threats, our predictive map of climate-induced camouflage mismatch (Fig. 4A) provides an initial framework for prioritizing conservation efforts. Adaptive potential may be enhanced through local management actions aimed at reducing anthropogenic stressors and promoting connectivity between populations harboring critical winter-brown variation. Our findings also enable quantification of color-associated variation in vulnerable populations using any DNA source without knowledge of winter phenotypes. In the absence of connectivity or standing variation,

our simulations suggest that local adaptation could be accelerated by modest amounts of human-assisted gene flow to mismatched populations (*44*).

Safeguarding the adaptive potential of populations is central for conservation (*1*), yet the genetic basis of adaptation is rarely incorporated into applied conservation planning (*11*, *45*). Landscape genomic approaches have proven useful for uncovering adaptive genetic variation and climate change vulnerability without knowledge of phenotypes (*46*, *47*). Our results show why a deeper understanding of the genetic basis of adaptive traits may also be needed to predict future responses of populations threatened by climate change and how such insights may be applied to facilitate evolutionary rescue.

References:

1. O. H. Frankel, M. E. Soulé, *Conservation and Evolution* (Cambridge University Press, Cambridge, 1981).
2. R. A. Bay, N. Rose, R. Barrett, L. Bernatchez, C. K. Ghalambor, J. R. Lasky, R. B. Brem, S. R. Palumbi, P. Ralph, Predicting responses to contemporary environmental change using evolutionary response architectures. *Am Nat*. **189**, 463–473 (2017).
3. M. Kardos, G. Luikart, The genetic architecture of fitness drives population viability during rapid environmental change. *Am. Nat.* **197** (2021), doi:10.1086/713469.
4. S. Lamichhaney, F. Han, J. Berglund, C. Wang, M. S. Almén, M. T. Webster, B. R. Grant, P. R. Grant, L. Andersson, A beak size locus in Darwin's finches facilitated character displacement during a drought. *Science* **352**, 470–474 (2016).

5. R. D. H. Barrett, S. Laurent, R. Mallarino, S. P. Pfeifer, C. C. Y. Xu, M. Foll, K. Wakamatsu, J. S. Duke-Cohan, J. D. Jensen, H. E. Hoekstra, Linking a mutation to survival in wild mice. *Science*. **363**, 499–504 (2019).

6. M. R. Jones, L. S. Mills, P. C. Alves, C. M. Callahan, J. M. Alves, D. J. R. Lafferty, F. M. Jiggins, J. D. Jensen, J. Melo-Ferreira, J. M. Good, Adaptive introgression underlies polymorphic seasonal camouflage in snowshoe hares. *Science*. **360**, 1355–1358 (2018).

7. M. Kardos, A. B. A. Shafer, The peril of gene-targeted conservation. *Trends Ecol Evol*. **33**, 827–839 (2018).

8. T. Q. Thompson, M. R. Bellinger, S. M. O'Rourke, D. J. Prince, A. E. Stevenson, A. T. Rodrigues, M. R. Sloat, C. F. Speller, D. Y. Yang, V. L. Butler, M. A. Banks, M. R. Miller, Anthropogenic habitat alteration leads to rapid loss of adaptive variation and restoration potential in wild salmon populations. *Proc. Natl. Acad. Sci.* **116**, 177–186 (2019).

9. J. M. Cohen, M. J. Lajeunesse, J. R. Rohr, A global synthesis of animal phenological responses to climate change. *Nat. Clim. Chang. 2018 8:3*. **8**, 224–228 (2018).

10. B. Helm, R. Ben-Shlomo, M. J. Sheriff, R. A. Hut, R. Foster, B. M. Barnes, D. Dominoni, Annual rhythms that underlie phenology: biological time-keeping meets environmental change. *Proc. R. Soc. B*. **280**, 20130016 (2013).

11. L. S. Mills, E. Bragina, A. V. Kumar, M. Zimova, J. Feltner, B. Davis, D. Lafferty, K. Häcklander, P. C. Alves, J. M. Good, J. Melo-Ferreira, A. Abramov, N. Lopatina, K. Fay, Winter coat color polymorphisms identify global hotspots for evolutionary rescue from climate change. *Science*. **359**, 1033–1036 (2018).

12. M. Zimova, L. S. Mills, J. J. Nowak, High fitness costs of climate change induced camouflage mismatch in a seasonally colour moulting mammal. *Ecol Lett*. **19**, 299–307 (2016).

13. E. C. Wilson, A. A. Shipley, B. Zuckerberg, M. Z. Peery, J. N. Pauli, An experimental translocation identifies habitat features that buffer camouflage mismatch in snowshoe hares. *Conserv Lett*. **12**, e12614 (2019).

14. L. S. Mills, M. Zimova, J. Oyler, S. Running, J. T. Abatzoglou, P. M. Lukacs, Camouflage mismatch in seasonal coat color due to decreased snow duration. *Proc Natl Acad Sci U S A*. **110**, 7360–7365 (2013).

15. K. Atmeh, A. Andruszkiewicz, K. Zub, Climate change is affecting mortality of weasels due to camouflage mismatch. *Sci Rep*. **8**, 1–7 (2018).

16. S. M. Sultaire, J. N. Pauli, K. J. Martin, M. W. Meyer, M. Notaro, B. Zuckerberg, Climate change surpasses land-use change in the contracting range boundary of a winter-adapted mammal. *Proc. R. Soc. B: Biol. Sci*. **283** (2016).

17. S. Pedersen, M. Odden, H. C. Pedersen, Climate change induced molting mismatch? Mountain hare abundance reduced by duration of snow cover and predator abundance. *Ecosphere*. **8**, e01722 (2017).

18. E. C. Wilson, B. Zuckerberg, M. Z. Peery, J. N. Pauli, The past, present and future impacts of climate and land use change on snowshoe hares along their southern range boundary *Biol. Conserv.* **249**, 108731 (2020).

19. D. E. Brown, A. T. Smith, J. K. Frey, B. R. Schweiger, A review of the ongoing decline of the white-tailed jackrabbit. *J Fish Wildl Manag*. **11**, 341–352 (2020).

20. R. M. Hansen, G. D. Bear, Winter coats of white-tailed jackrabbits in southwestern Colorado. *J. Mammology*. **44**, 420–422 (1963).

21. Supplementary Materials Online.

22. D. Enshell-Seijffers, C. Lindon, B. A. Morgan, The serine protease Corin is a novel modifier of the agouti pathway. *Development*. **135**, 217–225 (2007).

23. X. Xu, G. X. Dong, A. Schmidt-Küntzel, X. L. Zhang, Y. Zhuang, R. Fang, X. Sun, X. S. Hu, T. Y. Zhang, H. D. Yang, D. L. Zhang, L. Marker, Z. F. Jiang, R. Li, S. J. Luo, The genetics of tiger pelage color variations. *Cell Res*. **27**, 954–957 (2017).

24. E. Avigad Laron, E. Aamar, D. Enshell-Seijffers, The serine protease activity of Corin is required for normal pigment type switching. *J. Invest. Dermatol.* **139**, 257–259 (2019).

25. M. Takeo, W. Lee, P. Rabbani, Q. Sun, H. Hu, C. H. Lim, P. Manga, M. Ito, EdnrB governs regenerative response of melanocyte stem cells by crosstalk with Wnt signaling. *Cell Rep*. **15**, 1291–1302 (2016).

26. H. Li, L. Fan, S. Zhu, M. K. Shin, F. Lu, J. Qu, L. Hou, Epilation induces hair and skin pigmentation through an EDN3/EDNRB-dependent regenerative response of melanocyte stem cells. *Sci Rep*. **7**, 1–13 (2017).

27. K. Hosoda, R. E. Hammer, J. A. Richardson, A. G. Baynash, J. C. Cheung, A. Giaid, M. Yanagisawa, Targeted and natural (piebald-lethal) mutations of endothelin-B receptor gene produce megacolon associated with spotted coat color in mice. *Cell*. **79**, 1267–1276 (1994).

28. H. Kashiwagi, H. Ishimoto, S. ichiro Izumi, T. Seki, R. Kinami, A. Otomo, K. Takahashi, F. Kametani, N. Hirayama, E. Sasaki, T. Shiina, K. Sakabe, M. Mikami, Y. Kametani, Human PZP and common marmoset A2ML1 as pregnancy related proteins. *Sci. Rep. 2020 10:1*. **10**, 1–13 (2020).

29. C. Tayade, S. Esadeg, Y. Fang, B. A. Croy, Functions of alpha 2 macroglobulins in pregnancy. *Mol Cell Endocrinol*. **245**, 60–66 (2005).

30. R. Sayegh, J. T. Awwad, C. Maxwell, B. Lessey, K. Isaacson, Alpha 2-macroglobulin production by the human endometrium. *J Clin Endocrinol Metab*. **80**, 1021–1026 (1995).

31. M. Manceau, V. S. Domingues, R. Mallarino, H. E. Hoekstra, The developmental role of agouti in color pattern evolution. *Science*. **331**, 1062–1065 (2011).

32. I. Giska, L. Farelo, J. Pimenta, F. A. Seixas, M. S. Ferreira, J. P. Marques, I. Miranda, J. Letty, H. Jenny, K. Hackländer, E. Magnussen, J. Melo-Ferreira, Introgression drives repeated evolution of winter coat color polymorphism in hares. *Proc. Natl. Acad. Sci.* **116**, 24150–24156 (2019).

33. M. R. Jones, L. S. Mills, J. D. Jensen, J. M. Good, The origin and spread of locally adaptive seasonal camouflage in snowshoe hares. *Am Nat*. **196** (2020).

34. M. R. Jones, L. S. Mills, J. D. Jensen, J. M. Good, Convergent evolution of seasonal camouflage in response to reduced snow cover across the snowshoe hare range. *Evolution*. **74**, 2033–2045 (2020).

35. F. A. Seixas, P. Boursot, J. Melo-Ferreira, The genomic impact of historical hybridization with massive mitochondrial DNA introgression. *Genome Biol*. **19**, 1–20 (2018).

36. F. Seixas, thesis, University of Porto and University of Montpellier, Porto and Montpellier (2017).

37. M. S. Ferreira, M. R. Jones, C. M. Callahan, L. Farelo, Z. Tolesa, F. Suchentrunk, P. Boursot, L. S. Mills, P. C. Alves, J. M. Good, J. Melo-Ferreira, The legacy of recurrent introgression during the radiation of hares. *Syst Biol*. **70**, 593–607 (2021).

38. S. Joly, P. A. McLenachan, P. J. Lockhart, A statistical approach for distinguishing hybridization and incomplete lineage sorting. *Am Nat*. **174**, E54–E70 (2009).

39. M. Moest, S. M. Van Belleghem, J. E. James, C. Salazar, S. H. Martin, S. L. Barker, G. R. P. Moreira, C. Merot, M. Joron, N. J. Nadeau, F. M. Steiner, C. D. Jiggins, Selective

sweeps on novel and introgressed variation shape mimicry loci in a butterfly adaptive radiation. *PLoS Biol*. **18**, e3000597 (2020).

40. D. Charlesworth, Balancing selection and its effects on sequences in nearby genome regions. *PLoS Genet*. **2**, e64 (2006).

41. G. Pederson, S. Gray, C. Woodhouse, The unusual nature of recent snowpack declines in the North American Cordillera. *Science* **333**, 332–335 (2011).

42. C. R. Schwalm, S. Glendon, P. B. Duffy, RCP8.5 tracks cumulative CO2 emissions. *Proc. Natl. Acad. Sci.* **117**, 19656–19657 (2020).

43. J. Asin, D. Rejmanek, D. L. Clifford, A. B. Mikolon, E. E. Henderson, A. C. Nyaoke, M. Macías-Rioseco, N. Streitenberger, J. Beingesser, L. W. Woods, A. Lavazza, L. Capucci, B. Crossley, F. A. Uzal, Early circulation of rabbit haemorrhagic disease virus type 2 in domestic and wild lagomorphs in southern California, USA (2020–2021). *Transbound Emerg Dis*, 1–12 (2021).

44. S. N. Aitken, M. C. Whitlock, Assisted Gene Flow to Facilitate Local Adaptation to Climate Change. *Annu Rev Ecol Evol Syst*. **44**, 367–388 (2013).

45. J. C. Teixeira, C. D. Huber, The inflated significance of neutral genetic diversity in conservation genetics. *Proc. Natl. Acad. Sci.* **118**, e2015096118 (2021).

46. O. Razgour, B. Forester, J. B. Taggart, M. Bekaert, J. Juste, C. Ibáñez, S. J. Puechmaille, R. Novella-Fernandez, A. Alberdi, S. Manel, Considering adaptive genetic variation in climate change vulnerability assessment reduces species range loss projections. *Proc Natl Acad Sci U S A*. **116**, 10418–10423 (2019).

47. R. A. Bay, R. J. Harrigan, V. Le Underwood, H. L. Gibbs, T. B. Smith, K. Ruegg, Genomic signals of selection predict climate-driven population declines in a migratory bird. *Science*. **359**, 83–86 (2018).

48. H. Constable, R. Guralnick, J. Wieczorek, C. Spencer, A. T. Peterson, VertNet: A New Model for Biodiversity Data Sharing. *PLoS Biol*. **8**, e1000309 (2010).

49. GBIF.org, GBIF Home Page. (2020), (available at https://www.gbif.org).

50. Arctos, Arctos. Collaborative Collection Management Solution (2020), (available at arctosdb.org).

51. T. J. Thurman, tjthurman/wtjr_sdm (2022), , doi:https://doi.org/10.5281/zenodo.7373507.

52. M. E. Aiello-Lammens, R. A. Boria, A. Radosavljevic, B. Vilela, R. P. Anderson, spThin: An R package for spatial thinning of species occurrence records for use in ecological niche models. *Ecography*. **38**, 541–545 (2015).

53. S. E. Fick, R. J. Hijmans, WorldClim 2: new 1-km spatial resolution climate surfaces for global land areas. *Int. J. Climatol.* **37**, 4302–4315 (2017).

54. R. J. Hijmans, Raster: geographic data analysis and modeling (2020).

55. S. J. Phillips, M. Dudík, Modeling of species distributions with Maxent: New extensions and a comprehensive evaluation. *Ecography*. **31**, 161–175 (2008).

56. R. Muscarella, P. J. Galante, M. Soley-Guardia, R. A. Boria, J. M. Kass, M. Uriarte, R. P. Anderson, ENMeval: An R package for conducting spatially independent evaluations and estimating optimal model complexity for Maxent ecological niche models. *Methods Ecol Evol*. **5**, 1198–1205 (2014).

57. R. J. Hijmans, S. Phillips, J. Leathwick, J. Elith, Dismo: species distribution modeling (2017).

58. M. Nunome, G. Kinoshita, M. Tomozawa, H. Torii, R. Matsuki, F. Yamada, Y. Matsuda, H. Suzuki, Lack of association between winter coat colour and genetic population structure in the Japanese hare, *Lepus brachyurus* (Lagomorpha: Leporidae). *Biol* **111**, 761–776 (2014).

59. C. R. Linnen, E. P. Kingsley, J. D. Jensen, H. E. Hoekstra, On the origin and spread of an adaptive allele in deer mice. *Science* **325**, 1095–1098 (2009).

60. M. S. Ferreira, MafaldaSFerreira/wtjr_camouflage (2022), , doi:https://doi.org/10.5281/zenodo.7324926.

61. K. Bi, T. Linderoth, D. A. N. Vanderpool, J. M. Good, R. Nielsen, Unlocking the vault : next-generation museum population genomics. *Mol Ecol*. **22**, 6018–6032 (2013).

62. B. Shapiro, M. Hofreiter, *Ancient DNA: methods and protocols* (Humana Press, New York, 2012).

63. M. Meyer, M. Kircher, Illumina sequencing sibrary preparation for highly multiplexed target capture and sequencing. *Cold Spring Harb Protoc*. **2010** (2010).

64. M. Kircher, S. Sawyer, M. Meyer, Double indexing overcomes inaccuracies in multiplex sequencing on the Illumina platform. *Nucleic Acids Res*. **40**, 1–8 (2012).

65. A. W. Briggs, U. Stenzel, M. Meyer, J. Krause, M. Kircher, S. Pääbo, Removal of deaminated cytosines and detection of in vivo methylation in ancient DNA. *Nucleic Acids Res*. **38**, 1–12 (2010).

66. N. Rohland, D. Reich, Cost-effective, high-throughput DNA sequencing libraries for multiplexed target capture. *Genome Res*. **22**, 939–946 (2012).

67. M. Carneiro, C. J. Rubin, F. di Palma, F. W. Albert, J. Alföldi, A. M. Barrio, G. Pielberg, N. Rafati, S. Sayyab, J. Turner-Maier, S. Younis, S. Afonso, B. Aken, J. M. Alves, D. Barrell, G. Bolet, S. Boucher, H. A. Burbano, R. Campos, J. L. Chang, V. Duranthon, L. Fontanesi, H. Garreau, D. Heiman, J. Johnson, R. G. Mage, Z. Peng, G. Queney, C. Rogel-Gaillard, M. Ruffier, S. Searle, R. Villafuerte, A. Xiong, S. Young, K. Forsberg-Nilsson, J. M. Good, E. S. Lander, N. Ferrand, K. Lindblad-Toh, L. Andersson, Rabbit

genome analysis reveals a polygenic basis for phenotypic change during domestication. *Science*. **345**, 1074–1079 (2014).

68. N. I. Weisenfeld, V. Kumar, P. Shah, D. M. Church, D. B. Jaffe, Direct determination of diploid genome sequences. *Genome Res*. **27**, 757–767 (2017).

69. A. Gurevich, V. Saveliev, N. Vyahhi, G. Tesler, Genome analysis QUAST: quality assessment tool for genome assemblies. *Bioinformatics*. **29**, 1072–1075 (2013).

70. M. Manni, M. R. Berkeley, M. Seppey, F. A. Simão, E. M. Zdobnov, BUSCO Update: Novel and Streamlined Workflows along with Broader and Deeper Phylogenetic Coverage for Scoring of Eukaryotic, Prokaryotic, and Viral Genomes. *Mol Biol Evol*. **38**, 4647–4654 (2021).

71. F. Cabanettes, C. Klopp, D-GENIES: Dot plot large genomes in an interactive, efficient and simple way. *PeerJ*. **2018**, e4958 (2018).

72. A. Shumate, S. L. Salzberg, Liftoff: accurate mapping of gene annotations. *Bioinformatics*. **37**, 1639–1643 (2020).

73. M. Lawrence, W. Huber, H. Pagès, P. Aboyoun, M. Carlson, R. Gentleman, M. T. Morgan, V. J. Carey, Software for Computing and Annotating Genomic Ranges. *PLoS Comput Biol*. **9**, 1003118 (2013).

74. A. C. E. Darling, B. Mau, F. R. Blattner, N. T. Perna, Mauve: Multiple alignment of conserved genomic sequence with rearrangements. *Genome Res*. **14**, 1394–1403 (2004).

75. B. A. J. Sarver, S. Keeble, T. Cosart, P. K. Tucker, M. D. Dean, J. M. Good, Phylogenomic insights into mouse evolution using a pseudoreference approach. *Genome Biol Evol*. **9**, 726–739 (2017).

76. A. M. Bolger, M. Lohse, B. Usadel, Trimmomatic: a flexible trimmer for Illumina sequence data. *Bioinformatics*. **30**, 1–7 (2014).

77. J. Zhang, K. Kobert, T. Flouri, A. Stamatakis, PEAR: a fast and accurate Illumina Paired-End reAd mergeR. *Bioinformatics*. **30**, 614–620 (2014).

78. H. Li, Aligning sequence reads, clone sequences and assembly contigs with BWA-MEM. *arXiv preprint*. **arXiv:1303** (2013) (available at http://github.com/lh3/bwa.).

79. H. Li, B. Handsaker, A. Wysoker, T. Fennell, J. Ruan, N. Homer, G. Marth, G. Abecasis, R. Durbin, The sequence alignment/map format and SAMtools. *Bioinformatics*. **25**, 2078–2079 (2009).

80. G. van der Auwera, B. O'Connor, an O. M. Company. Safari, Genomics in the Cloud: Using Docker, GATK, and WDL in Terra. *Genomics in the Cloud*, 300 (2020).

81. K. Okonechnikov, A. Conesa, F. García-Alcalde, Qualimap 2: Advanced multi-sample quality control for high-throughput sequencing data. *Bioinformatics*. **32**, 292–294 (2016).

82. T. S. Korneliussen, A. Albrechtsen, R. Nielsen, ANGSD: analysis of next generation sequencing data. *BMC Bioinformatics*. **15**, 1–13 (2014).

83. S. Y. Kim, K. E. Lohmueller, A. Albrechtsen, Y. Li, T. Korneliussen, G. Tian, N. Grarup, T. Jiang, G. Andersen, D. Witte, T. Jorgensen, T. Hansen, O. Pedersen, J. Wang, R. Nielsen, Estimation of allele frequency and association mapping using next-generation sequencing data. *BMC Bioinformatics*. **12**, 1–16 (2011).

84. H. Li, A statistical framework for SNP calling, mutation discovery, association mapping and population genetical parameter estimation from sequencing data. *Bioinformatics*. **27**, 2987–2993 (2011).

85. S. Purcell, B. Neale, K. Todd-Brown, L. Thomas, M. A. R. Ferreira, D. Bender, J. Maller, P. Sklar, P. I. W. de Bakker, M. J. Daly, P. C. Sham, PLINK: A tool set for whole-genome association and population-based linkage analyses. *Am J Hum Genet*. **81**, 559–575 (2007).

86. L. Skotte, T. S. Korneliussen, A. Albrechtsen, Estimating individual admixture proportions from next generation sequencing data. *Genetics*. **195**, 693–702 (2013).

87. G. Evanno, S. Regnaut, J. Goudet, Detecting the number of clusters of individuals using the software STRUCTURE: A simulation study. *Mol Ecol*. **14**, 2611–2620 (2005).

88. R. Nielsen, T. Korneliussen, A. Albrechtsen, Y. Li, J. Wang, SNP calling, genotype calling, and sample allele frequency estimation from new-generation sequencing data. *PLoS One*. **7**, e37558 (2012).

89. L. Skotte, T. S. Korneliussen, A. Albrechtsen, Association testing for next-generation sequencing data using score statistics. *Genet Epidemiol*. **36**, 430–437 (2012).

90. P. Cingolani, A. Platts, L. L. Wang, M. Coon, T. Nguyen, L. Wang, S. J. Land, X. Lu, D. M. Ruden, A program for annotating and predicting the effects of single nucleotide polymorphisms, SnpEff. *Fly* **6**, 80–92 (2012).

91. J. Meisner, A. Albrechtsen, Inferring population structure and admixture proportions in low-depth NGS data. *Genetics*. **210**, 719–731 (2018).

92. S. A. Sefick, M. A. Castronova, L. S. Stevison, genotypeR: An integrated r package for single nucleotide polymorphism genotype marker design and data analysis. *Methods Ecol Evol*. **9**, 1318–1323 (2018).

93. S. Chen, Y. Zhou, Y. Chen, J. Gu, fastp: an ultra-fast all-in-one FASTQ preprocessor. *Bioinformatics*. **34**, i884–i890 (2018).

94. P. Danecek, J. K. Bonfield, J. Liddle, J. Marshall, V. Ohan, M. O. Pollard, A. Whitwham, T. Keane, S. A. McCarthy, R. M. Davies, H. Li, Twelve years of SAMtools and BCFtools. *Gigascience*. **10** (2021).

95. G. Bhatia, N. Patterson, S. Sankararaman, A. L. Price, Estimating and interpreting F ST : The impact of rare variants, *Genome Res.* **23, 1514–1521**.

96. T. Wei, V. Simko, R package "corrplot": Visualization of a Correlation Matrix (Version 0.92).

97. T. Magoč, S. L. Salzberg, FLASH: Fast length adjustment of short reads to improve genome assemblies. *Bioinformatics*. **27**, 2957–2963 (2011).

98. A. R. Quinlan, I. M. Hall, BEDTools: a flexible suite of utilities for comparing genomic features. *Bioinformatics*. **26**, 841–842 (2010).

99. M. L. Borowiec, AMAS: A fast tool for alignment manipulation and computing of summary statistics. *PeerJ*. **2016**, e1660 (2016).

100. A. Stamatakis, RAxML version 8: a tool for phylogenetic analysis and post-analysis of large phylogenies. *Bioinformatics*. **30**, 1312–1313 (2018).

101. L.-T. Nguyen, H. A. Schmidt, A. von Haeseler, B. Q. Minh, IQ-TREE: a fast and effective stochastic algorithm for estimating maximum-likelihood phylogenies. *Mol Biol Evol*. **32**, 268–274 (2015).

102. S. Kalyaanamoorthy, B. Q. Minh, T. K. F. Wong, A. von Haeseler, L. S. Jermiin, ModelFinder: Fast model selection for accurate phylogenetic estimates. *Nat Methods*. **14**, 587–589 (2017).

103. D. Thi Hoang, O. Chernomor, A. von Haeseler, B. Quang Minh, L. Sy Vinh, M. S. Rosenberg, UFBoot2: improving the ultrafast bootstrap approximation. *Mol. Biol. Evol.* **35**, 518–522 (2017).

104. S. Guindon, J.-F. Dufayard, V. Lefort, M. Anisimova, W. Hordijk, O. Gascuel, New algorithms and methods to estimate maximum-likelihood phylogenies: assessing the performance of PhyML 3.0. *Syst Biol*. **59**, 307–321 (2010).

105. C. Zhang, M. Rabiee, E. Sayyari, S. Mirarab, ASTRAL-III: Polynomial time species tree reconstruction from partially resolved gene trees. *BMC Bioinformatics*. **19**, 15–30 (2018).

106. R. Bouckaert, T. G. Vaughan, J. Barido-Sottani, S. Duchêne, M. Fourment, A. Gavryushkina, J. Heled, G. Jones, D. Kühnert, N. de Maio, M. Matschiner, F. K. Mendes, N. F. Müller, H. A. Ogilvie, L. du Plessis, A. Popinga, A. Rambaut, D. Rasmussen, I. Siveroni, M. A. Suchard, C. H. Wu, D. Xie, C. Zhang, T. Stadler, A. J. Drummond, BEAST 2.5: An advanced software platform for Bayesian evolutionary analysis. *PLoS Comput Biol*. **15**, e1006650 (2019).

107. C. Matthee, B. van Vuuren, D. Bell, T. Robinson, A molecular supermatrix of the rabbits and hares (Leporidae) allows for the identification of five intercontinental exchanges during the Miocene. *Syst Biol*. **53**, 433–447 (2004).

108. A. Rambaut, A. J. Drummond, D. Xie, G. Baele, M. A. Suchard, Posterior summarization in Bayesian phylogenetics using Tracer 1.7. *Syst Biol*. **67**, 901–904 (2018).

109. S. H. Martin, S. M. van Belleghem, Exploring evolutionary relationships across the genome using topology weighting. *Genetics*. **206**, 429–438 (2017).

110. B. K. Rosenzweig, J. B. Pease, N. J. Besansky, M. W. Hahn, Powerful methods for detecting introgressed regions from population genomic data. *Mol Ecol*. **25**, 2387–2397 (2016).

111. R. E. Green, J. Krause, A. W. Briggs, T. Maricic, U. Stenzel, M. Kircher, N. Patterson, H. Li, W. Zhai, M. H.-Y. Fritz, N. F. Hansen, E. Y. Durand, A.-S. Malaspinas, J. D. Jensen, T. Marques-Bonet, C. Alkan, K. Prüfer, M. Meyer, H. A. Burbano, J. M. Good, R. Schultz, A. Aximu-Petri, A. Butthof, B. Höber, B. Höffner, M. Siegemund, A. Weihmann, C. Nusbaum, E. S. Lander, C. Russ, N. Novod, J. Affourtit, M. Egholm, C. Verna, P. Rudan, D. Brajkovic, Ž. Kucan, I. Gušic, V. B. Doronichev, L. v Golovanova, C. Lalueza-Fox, M. de la Rasilla, J. Fortea, A. Rosas, R. W. Schmitz, P. L. F. Johnson, E. E. Eichler, D. Falush, E. Birney, J. C. Mullikin, M. Slatkin, R. Nielsen, J. Kelso, M. Lachmann, D. Reich, S. Pääbo, A draft sequence of the Neandertal genome. *Science*. **328**, 710–722 (2010).

112. S. H. Martin, J. W. Davey, C. D. Jiggins, Evaluating the use of ABBA-BABA statistics to locate introgressed loci. *Mol Biol Evol*. **32**, 244–257 (2015).

113. I. Gronau, M. J. Hubisz, B. Gulko, C. G. Danko, A. Siepel, Bayesian inference of ancient human demography from individual genome sequences. *Nat Genet*. **43**, 1031–1035 (2011).

114. G. Ewing, J. Hermisson, J. Barrett, MSMS: a coalescent simulation program including recombination, demographic structure and selection at a single locus. *Bioinformatics*. **26**, 2064–2065 (2010).

115. T. E. Cruickshank, M. W. Hahn, Reanalysis suggests that genomic islands of speciation are due to reduced diversity, not reduced gene flow. *Mol Ecol*. **23**, 3133–3157 (2014).

116. B. C. Haller, P. W. Messer, SLiM 3: Forward Genetic Simulations Beyond the Wright–Fisher Model. *Mol Biol Evol*. **36**, 632–637 (2019).

117. B. W. Brook, J. J. O'Grady, A. P. Chapman, M. A. Burgman, H. Resit Akçakaya, R. Frankham, Predictive accuracy of population viability analysis in conservation biology. *Nature 2000 404:6776*. **404**, 385–387 (2000).

118. R. Lande, Risks of Population Extinction from Demographic and Environmental Stochasticity and Random Catastrophes. *Am Nat*. **142**, 911–927 (1993).

119. T. R. James, R. W. Seabloom, Reproductive Biology of the White-Tailed Jack Rabbit in North Dakota. *J Wildl Manage*. **33**, 558–568 (1969).

120. M. T. Simes, K. M. Longshore, K. E. Nussear, G. L. Beatty, D. E. Brown, T. C. Esque, Black-tailed and white-tailed jackrabbits in the American West: History, ecology, ecological significance, and survey methods. *West N Am Nat*. **75**, 491–519 (2015).

121. IUCN (International Union for Conservation of Nature) 2008. Lepus townsendii. The IUCN Red List of Threatened Species. Version 3.1. https://www.iucnredlist.org. Downloaded on 24 May 2022.

Acknowledgments: L. Rossier, T. Williams, N. Herrera, B. Davis, E. Larson, J. Sweatman, M. McLaughlin, USDA Wildlife Services (North and South Dakota), and Colorado Parks and

Wildlife (Gunnison and Monte Vista) assisted in sample collection. We thank L. Olson, E. Braker, E. Rickart, A. Hornsby, E. Westwig, N. Duncan, A. Doll and J. Stephenson for access to museum collections and R. Wicker for specimen photographs. We thank P. Boursot, J. Jensen, M. Kardos, members of EVOCHANGE, the UNVEIL Network, CIBIO-InBIO, T. Wheeler and the UM Genomics Core for helpful discussions and experimental support. Sequencing was performed at Novogene Technology Co., Ltd (Davis, CA) and UC Davis Genome Center (Davis, CA). Computational resources were provided by Griz Shared Computing Cluster and CIBIO New-Gen platform.

Funding:

National Science Foundation (NSF), EPSCoR grant (OIA-1736249) (JMG).

Fundação para a Ciência e a Tecnologia (FCT), "2CHANGE" PTDC/BIA-EVL/28124/2017, co-funded by ERDF through COMPETE 2020 POCI-01-0145-FEDER-028124 (JM-F).

FCT, PhD grant PD/BD/108131/2015 (POPH-QREN funds from ESF and Portuguese MCTES/FCT) (MSF).

FCT, 2021.00150.CEECIND (JM-F).

NSF, DEB-1907022 (LSM, JMG), DGE-1702043 (MRJ), DGE-1313190 (LSM), and PRFB-1907243 (TJT).

Society for the Study of Evolution, Rosemary Grant Graduate Student Research Award (MSF).

European Society for Evolutionary Biology, Godfrey Hewitt Mobility Award (MSF).

Fundação Luso-Americana para o Desenvolvimento, Portugal-United States of America Research Networks Program (MSF, PCA).

European Union's Seventh Framework Programme, grant no. 286431 (CIBIO New-Gen sequencing platform).

National Institutes of Health Shared Instrumentation Grant 1S10OD010786-01 (UC Davis Genome Center).

Author contributions:

Conceptualization: MSF, LSM, PCA, JM-F, JMG

Supervision: JM-F, JMG

Data Curation: MSF, TJT

Validation: MSF, TJT

Investigation: MSF, TJT, PCA, JMG, MRJ, LF, SMEM

Formal Analysis: MSF, TJT, AVK

Resources: LSM, JRD, JM-F, JMG

Funding acquisition: MSF, LSM, PCA, MRJ, TJT, JM-F, JMG

Visualization: MSF, TJT, JM-F, JMG

Writing – original draft: MSF, JM-F, JMG

Writing – review & editing: All Authors

Competing interests: None declared.

Data and materials availability: Sequence data are available in NCBI (BioProject PRJNA726805, SAMN19037327-SAMN19037409, SAMN30246380-SAMN30246447;

BioProjects PRJNA420081, PRJNA242290, PRJNA399194, PRJNA561428, PRJNA564335; Data S1). Genotype, spectrophotometry data and the annotated *L. townsendii* reference genome are deposited in Figshare (https://figshare.com/s/0a2dce1d3a6cf15d0e3d) and NCBI (PRJNA729659, PRJNA729660). Analysis code and related resources are archived in Zenodo (https://doi.org/10.5281/zenodo.7324926, https://doi.org/10.5281/zenodo.7373507).

Supplementary Materials

Materials and Methods

Figs. S1 to S18

Tables S1 to S14

Data S1 to S4

References (48-121)

Fig. 1. Winter coat color variation in white-tailed jackrabbits. (A) Probability of winter-brown coats across the modeled white-tailed jackrabbit distribution. **(B)** Representative winter coat color variation (Photo credit: Denver Museum of Nature & Science). **(C)** Sampling locations used for association mapping across Colorado, scaled by sample size.

Fig. 2. The genetic basis of winter coat color variation. (A) Genome-wide associations ($-\log_{10}$ *P* values; 5,557,716 SNPs) with winter coat color (inset: dorsal photos ordered by PC1) of 61 jackrabbits (dashed line, Bonferroni-corrected $P=0.05$). Local associations, gene structures, and dorsal reflectance across assayed diploid genotypes (BB=homozygous brown; BW=heterozygous;

WW=homozygous white) for *CORIN* **(B, C)** and *EDNRB* **(D, E)**. Significant associations are highlighted in dark blue (Bonferroni-corrected $P \leq 0.05$). **(F)** Dorsal images of specimens with double homozygous or heterozygous *CORIN* and *EDNRB* genotypes.

Fig. 3. Evolution of winter coat color variation. (A) Scaled absolute genetic divergence (RND) in 20-kb sliding windows (dots, 2-kb step size) between one homozygous winter-white and winter-brown genome. Association intervals are gray, orange dots are windows of elevated divergence (RND Z-score ≥ 3), and gaps represent missing data in the reference assembly. **(B)** Phylogenies of *CORIN, EDNRB* and *ASIP* (associated intervals) differed from the multispecies coalescent tree (43,430 50-kb windows, Fig. S11). (*) denotes species where winter pelage variation has previously been associated with introgression (*6*, *33*). Branches with bootstrap support <80 are labeled. Empirical and simulated distributions of genetic divergence (d_{xy}) genome-wide, for *CORIN, EDNRB*, and *ASIP* between white-tailed jackrabbits and **(C)** black-tailed jackrabbits or **(D)** Arctic hares.

Fig. 4. Adaptation to future climate-induced mismatch. (A) Predicted phenotypic mismatch ($\Delta P_{(brown)}$) in 2080 using RCP8.5 forecasts of snow residence time, mean diurnal temperature range, and isothermality (inset: predicted probability shifts towards winter-brown across the USA range). **(B)** Simulated size trajectories of populations (30 replicates; line = averages, ribbons = 95% quantiles) experiencing future camouflage mismatch ($\Delta P_{(brown)} = 0.75$) shown as a proportion of the population ceiling (dotted line) assuming standing variation of additive (left panel) or recessive (right panel) brown alleles at *CORIN* and *EDNRB*.

Figure 1

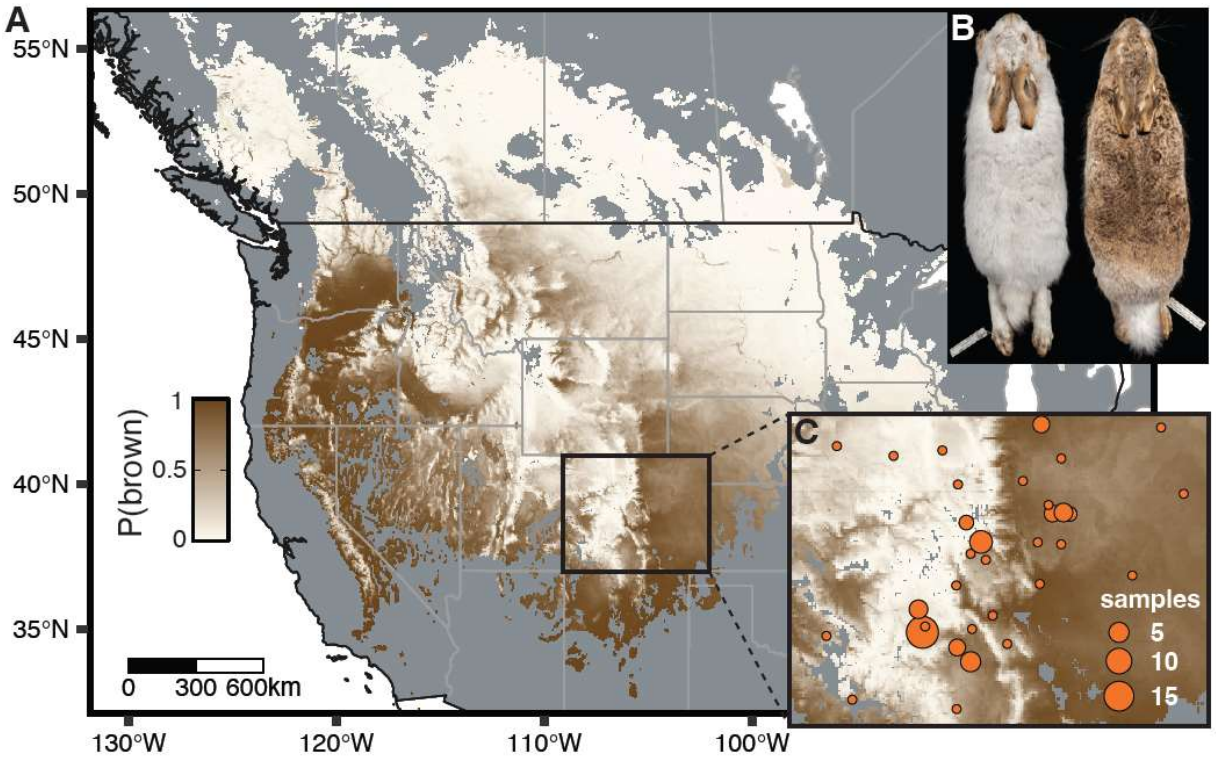

Figure 2

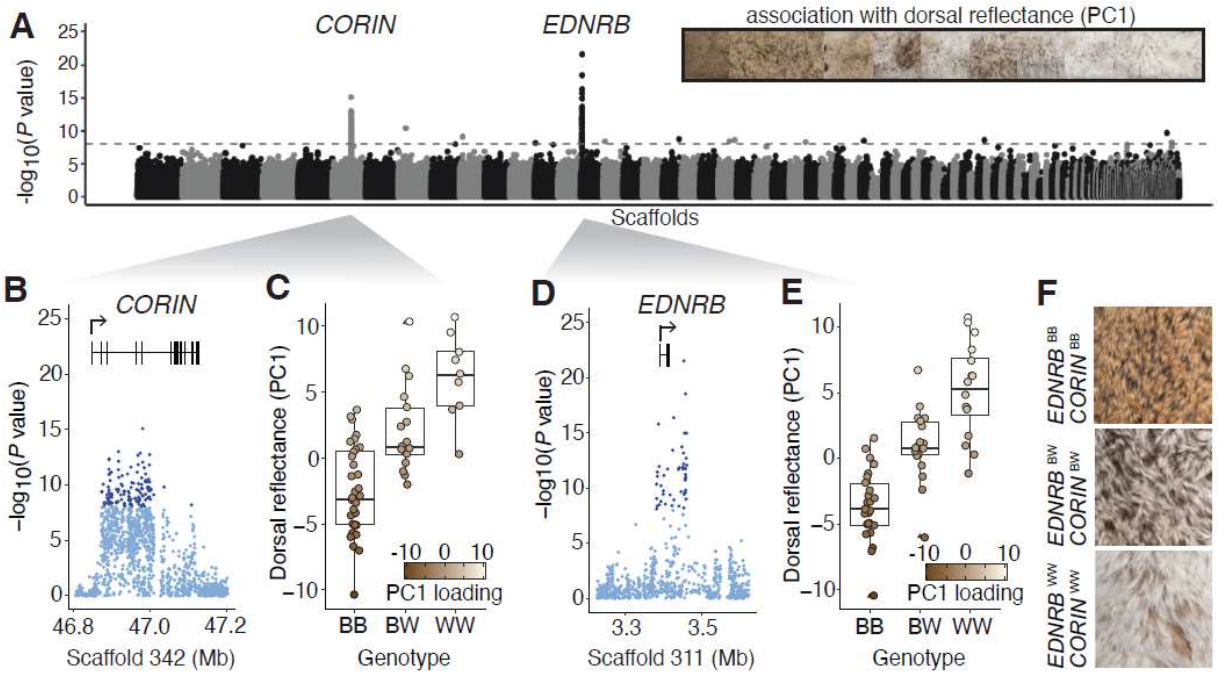

Figure 3

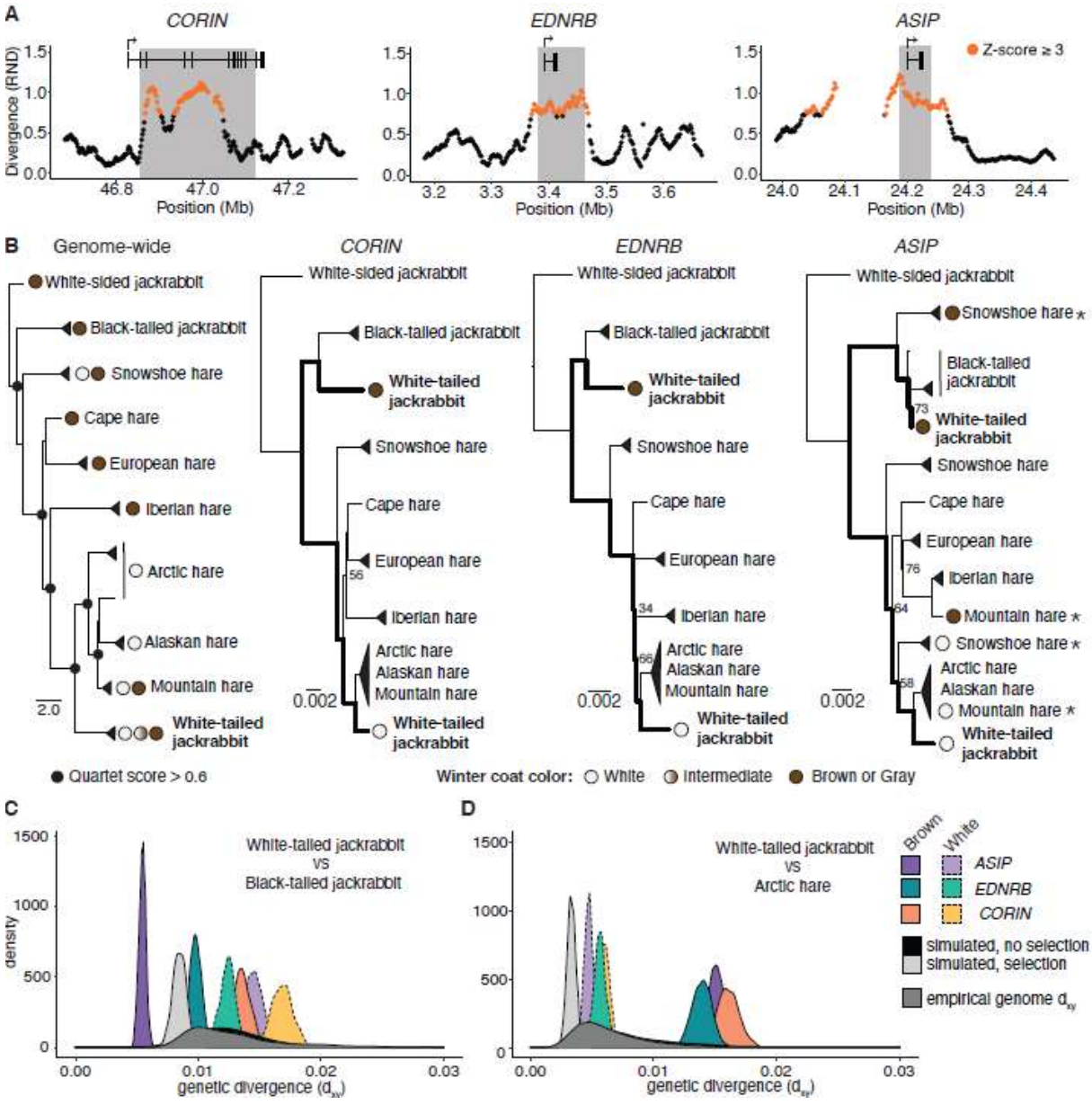

Figure 4